Degree of disorder in cubic mesophases in thermotropics: Thermodynamic study of a liquid crystal showing two cubic mesophases

Kazuya Saito,[1,*] Takashi Shinhara,[1] Tadahiro Nakamoto,[1] Shoichi Kutsumizu,[2,†] Shinichi Yano,[3] and Michio Sorai[1]
[1]*Research Center for Molecular Thermodynamics, Graduate School of Science, Osaka University, Toyonaka, Osaka 560-0043, Japan*
[2]*Instrumental Analysis Center, Gifu University, Gifu 501-1193, Japan*
[3]*Faculty of Engineering, Gifu University, Gifu 501-1193, Japan*
(Received 13 June 2001; published 6 March 2002)

Heat capacity of a thermotropic mesogen ANBC(22) (4′-alkoxy-3′-nitrobiphenyl-4-carboxylic acid with 22 carbon atoms in alkyl chain) showing two cubic mesophases was measured by adiabatic calorimetry between 13 and 480 K. Excess enthalpies and entropies due to phase transitions were determined. A small thermal anomaly due to the cubic *Im3m*→cubic *Ia3d* phase transition was successfully detected. Through an analysis of chain-length dependence of the entropy of transition, the sequence of two cubic mesophases (with space groups *Ia3d* and *Im3m*) is deduced for thermotropic mesogens ANBC(n). It is shown that the disorder of the core arrangement decreases in the order of Sm-C→cubic (*Im3m*)→cubic (*Ia3d*) while that of the chain in the reverse order cubic (*Ia3d*)→cubic (*Im3m*)→Sm C.

DOI: 10.1103/PhysRevE.65.031719 PACS number(s): 64.70.Md, 61.30.Gd, 65.20.+w

I. INTRODUCTION

Bicontinuous labyrinth, formed by dividing space by a periodic minimal surface, with high space group symmetry such as *Ia3d* or *Im3m* is one of the most exotic structures that nature forms. This type of structure is seen in thermotropic and lyotropic liquid crystals [1,2] and in block copolymers [3]. Its scale is much longer than molecular length but much shorter than macroscopic scale. Although models approached from the bulk side considering interface or surface exist, those from the molecular side are scarce. This situation is especially unfavorable for thermotropic liquid crystals, because it is hard to find the ''surface'' in the system. Construction of molecular model, which will contribute to our understandings not only for thermotropics but also for multicomponent systems, is therefore strongly desired.

Statistical modeling of liquid crystals goes back to Onsager [4], who assumed that mesogenic molecules are well approximated by hard rods. Many succeeding theories have also assumed rigid bodies as molecules [5,6]. Most mesogenic molecules, however, are not rigid but consist of rigid core and flexible alkyl chain(s). This situation has prevented quantitative comparison between predictions by models and experimental results. On the other hand, there is no experimental methodology widely accepted to deduce thermodynamic quantities that are suitable for direct comparisons with models. In this context, the status of the field is still insufficient from both theoretical and experimental sides.

Cubic mesophases in thermotropic liquid crystal usually appear in between liquid crystalline phases. Most cubic mesophases are believed to have a labyrinth structure characterized by a space group either *Ia3d* or *Im3m*. Only a slight modification of molecule influences the choice between *Ia3d* and *Im3m*. For example, the first two cubic mesogens ANBC(n) (4′-n-alkoxy-3′-nitrobiphenyl-4-carboxylic acid; n in the parenthesis being the number of carbon atoms in the alkyl chain; see Fig. 1) [7,8] and ACBC(n) (4′-n-alkoxy-3′-cyanobiphenyl-4-carboxylic acid) [9] exhibit the cubic phases with *Ia3d* and *Im3m*, respectively [10]. The thermodynamic (i.e., statistical mechanical) relation between the two phases has not been known. Here, we derive in a simple and reasonable method to assess the degree of disorder among two cubic phases and the neighboring Sm-C phase (smectic-C phase; layered structure with a tilted director

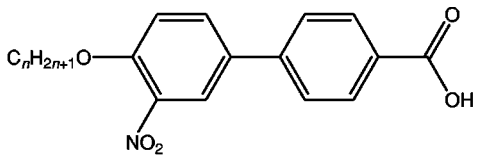

ANBC(n)

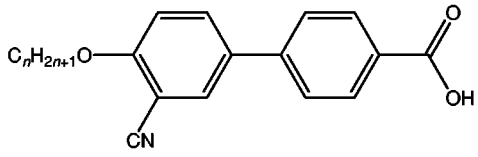

ACBC(n)

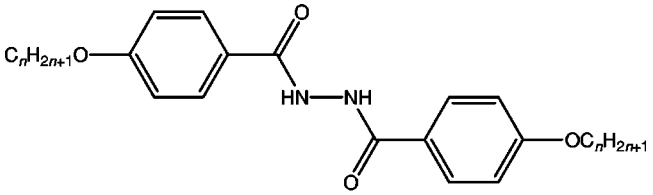

BABH(n)

FIG. 1. Molecular structures of ANBC(n), ACBC(n), and BABH(n).

*Corresponding author.
†Present address: Faculty of Engineering, Gifu University.

with respect to the layer normal) at the microscopic level, by extending our analysis of the most macroscopic quantity, entropy of transition. This idea will surely serve as a framework of molecular-statistical modeling of the cubic mesophases, and hopefully as a guide to clarify thermodynamic stability of exotic labyrinth structures in the nature.

In a previous study, Saito *et al.* [11] showed that the cubic phase of ANBC may be regarded as a binary system consisting of rigid (dimerized) core and flexible alkyl chains. On that basis, the degree of disorder of both the ''components'' was deduced for the *Ia3d* and Sm-*C* phases in terms of entropy [12,13]. Also shown was that the ''binary mixture'' picture is applicable to other cubic mesogens [14]. The phase behavior is primarily governed by the number of paraffinic carbon atoms in the system, i.e., the fraction of the chain ''component'' [15]. This successful ''binary mixture'' picture is also a basis of this paper.

Recently, Kutsumizu and co-workers [16–18] found two cubic phases in one and the same ANBC(n) with $n \geqslant 22$ in the phase sequence of Sm-$C \rightarrow$cubic (*Im3m*) $\rightarrow$cubic (*Ia3d*) on increasing the temperature. This series of compounds thus open a possibility to explore the relation between two cubic mesophases. Detection of a thermal anomaly between the two cubic phases in ANBC(22) was hard by a commercial instrument. In this paper, the results of the precise adiabatic calorimetry on ANBC(22) are reported, and the degree of disorder will be experimentally deduced for the Sm-*C*, *Ia3d*, and *Im3m* cubic phases.

II. EXPERIMENT

The sample of ANBC(22) was synthesized according to the literature [9] at Gifu University. Elemental analysis yielded the following results: C 73.86% (calculated 74.03%), H; 9.47% (9.41%); and N, 2.59% (2.47%). A powder sample was loaded in a beaker made of fused quartz to avoid direct contact with the metal surface of the gold-plated calorimeter vessel made of copper-beryllium alloy, which may catalyze decomposition. The beaker was settled in the vessel, which was sealed by use of a lead gasket vacuum tight after introducing a small amount of helium gas (20 kPa at room temperature) to aid thermal equilibration inside the vessel. The mass of the sample loaded into the vessel was 2.1699 g (3.8215 mmol).

The heat capacity was measured at Osaka University by using an adiabatic calorimeter, the details of which are described elsewhere [19]. The temperature scale employed was the IPTS-68, which is sufficiently precise for the purpose of the present study [20].

III. RESULTS AND DISCUSSION

A. Heat capacity and thermodynamic functions

Due to an accident that happened in the calorimetry system, the sample was unexpectedly heated up to ca. 360 K, where ANBC(22) is in Sm-*C* phase, prior to the measurement. Differential scanning calorimetry and x-ray experiments showed that the crystal polymorph of ANBC(22) obtained from melt is different from that of as-prepared sample.

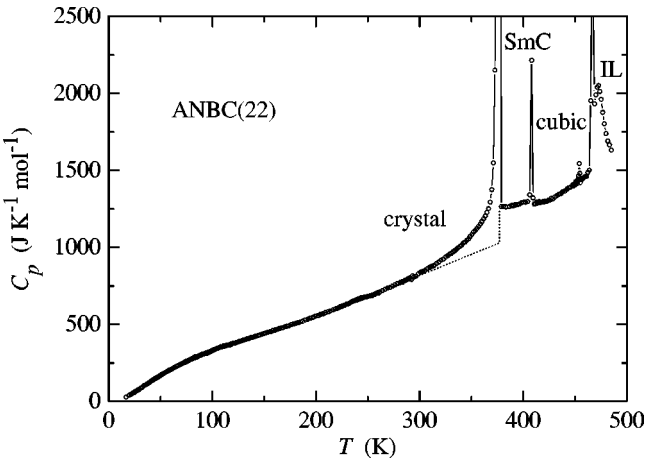

FIG. 2. Measured heat capacities of ANBC(22) in the whole temperature range. The isotropic liquid is denoted by IL. The assumed normal heat capacity (baseline) is drawn by a dotted curve.

Heat capacity of ANBC(22) was measured between 13 and 480 K by adiabatic calorimetry. The time required for thermal equilibration was within 20 min below 30 K, 30 min at 100 K, 20 min at 200 K, and 30 min at 300 K outside the transition region. In the transition region, the thermal relaxation time was significantly and abruptly prolonged as the transition temperature was approached. The longest time used for monitoring the temperature drift was, however, 120 min in these experiments for the practical reason. This truncation obviously has influence on the resultant data of apparent heat capacity but no effect on the integrated enthalpy change because of the first law of thermodynamics.

The sample contributed about 20% to the total heat capacity including those of the beaker and vessel over the temperature range studied. The heat capacity values reported in this paper are reliable within $\pm 0.1\%$ above 50 K [19].

Typical data are shown in Fig. 2 for the whole temperature range. Temperature increment due to each energy input was smaller than 2 K or 1% of temperature. By integrating the experimental heat capacities with respect to T and $\ln T$, standard enthalpy, entropy, and thus Gibbs energy were calculated. Standard thermodynamic quantities at round temperatures were deposited as a part of the EPAPS (Electronic Physics Auxiliary Publication Service) material [21], which also contains the primary heat capacity data.

B. Phase transitions

Within the temperature range covered by the present measurements, there exist six phases. Phase transitions between them occur above room temperature. Although it cannot be recognized in Fig. 2, the metastable crystalline phase (CrI′ in Table I) undergoes a phase transition at 375.69 K with the latent heat of about 30 kJ mol^{-1} to other crystalline phase (CrII′) as shown in Fig. 3. Since this phase transition has an appreciable tail at the low-temperature side, the estimate of the excess enthalpy and entropy associated with this transition requires determination of a baseline, which will be done in the following section.

TABLE I. Thermodynamic quantities of ANBC(22) associated with the phase transitions and the thermal anomaly appearing in the isotropic liquid state.

Transition	T_{trs} (K)	$\Delta_{trs}H$ (kJ mol^{-1})	$\Delta_{trs}S$ (J K^{-1} mol^{-1})
CrI′→CrII′	375.69	37.62	101.89
CrII′→Sm*C*	377.04	36.34	96.41
Sm*C*→*Im3m*	407.91	1.98	4.84
Im3m→*Ia3d*	454.13	0.17	0.37
Ia3d→IL [a]	466.76	4.03	8.64
Anomaly in IL [a]	~475	5.6	11.8

[a]Isotropic liquid.

The liquid crystalline Sm-*C* phase appears on melting at 377.04 K. The enthalpy (latent heat) and entropy of melting are estimated to be 36.34 kJ mol^{-1} and 96.41 J K^{-1} mol^{-1}, respectively. On further heating, a phase transition from the Sm-*C* phase to a cubic mesophase with space group *Im3m* occurs at 407.91 K as seen in Fig. 4. The enthalpy and entropy of transition are estimated to be 1.98 kJ mol^{-1} and 4.84 J K^{-1} mol^{-1}, respectively, while assuming the temperature dependences of the normal heat capacities of the Sm-*C* and the cubic phases being quadratic.

The cubic (*Im3m*)→cubic (*Ia3d*) transition takes place at 454.13 K as shown in Fig. 5. The anomaly is much smaller than that at the Sm-*C*→cubic transition at 407.91 K. Indeed, the enthalpy and entropy of transition are estimated as 0.17 kJ mol^{-1} and 0.37 J K^{-1} mol^{-1}, respectively, which are less than one-tenth of those values observed for usual liquid crystalline phase transitions. According to Landau's phenomenological theory of phase transition based on group theoretical consideration [22], this transition (between space groups *Ia3d* and *Im3m*) cannot be of higher order (continuous) [23]. That is, it should be of first order though the thermal anomaly is small. The thermodynamic quantities associated with the present phase transitions are summarized in Table I.

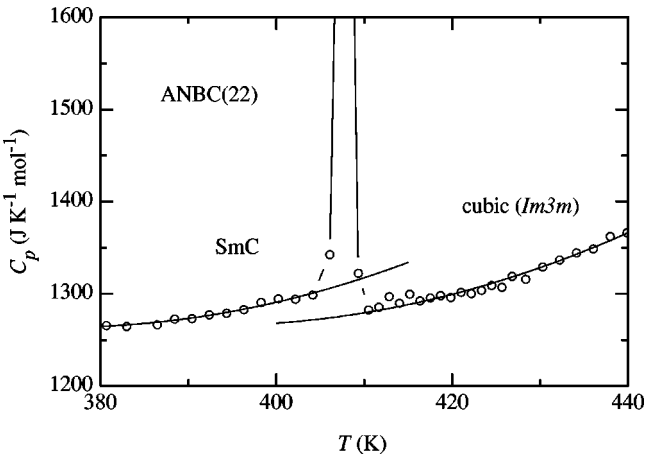

FIG. 4. Measured heat capacities of ANBC(22) around the Sm-*C*→cubic (*Im3m*) transition. Solid curves are smooth extrapolations of the heat capacities of the Sm-*C* and cubic phases.

A large heat capacity hump was observed in the isotropic liquid state as seen in Fig. 2. Assuming the constant value of 1502 J K^{-1} mol^{-1} for a normal heat capacity of the isotropic liquid, the enthalpy and entropy associated with this hump are estimated as 5.6 kJ mol^{-1} and 11.8 J K^{-1} mol^{-1}, respectively. The hump of heat capacity in the isotropic liquid region has been widely observed in the homologous series of ANBC [24]. Similar broad humps have also been reported for some liquid crystalline substances at the temperatures above destruction of a higher-order structure. As a possible cause for the hump, destruction of shorter-range order than the original unit length has been suggested [25]. For the binary systems between ANBCs and *n*-tetradecane, Saito *et al.* [11] reported that the hump appears even in the systems having no cubic phase and that the hump is enhanced as the number of paraffinic carbon atoms in the binary systems is increased. This trend was interpreted by assuming that the hump is due to the dissociation of ANBC dimer [24] and that the growth originates in the entropy effect. The excess enthalpy in ANBC(22) is also compatible with dissociation of carboxylic dimer [26,27]. A comparison between the experi-

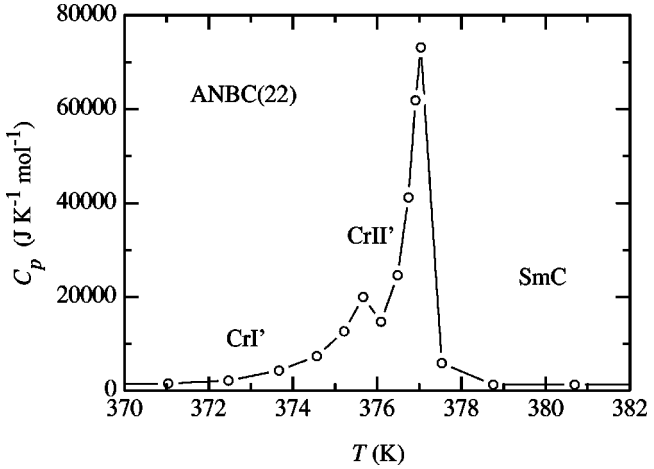

FIG. 3. Measured heat capacities of ANBC(22) in the melting region. Two crystalline phases are denoted by CrI′ and CrII′.

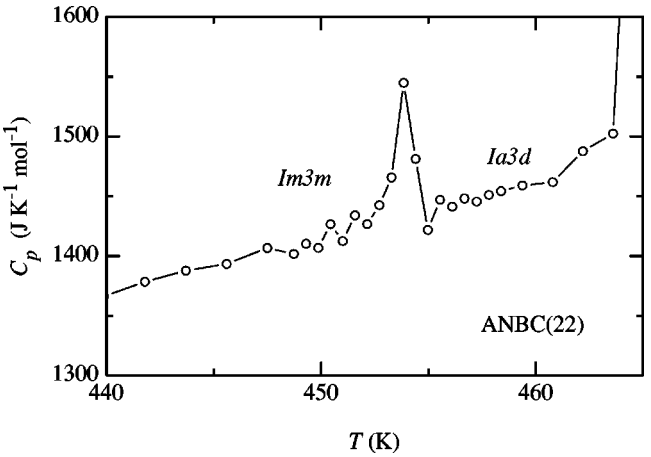

FIG. 5. Measured heat capacities of ANBC(22) around cubic (*Im3m*)→cubic (*Ia3d*) transition.

mental and calculated heat capacities using the temperature evolution of the fraction of ANBC(16) molecule participating dimer formation (as a function of temperature) [28], however, clearly showed that some cooperative mechanism be involved for full account of the hump. A narrow width of the hump implies that this is also the case for the present compound.

C. Configurational disorder of alkyl chain

The cubic mesogens ANBC(16) [26], ANBC(18) [12], and BABH(8) [1,2,-bis(4-*n*-alkyloxybenzoyl)hydrazine, Fig. 1] [29–31], commonly exhibit large solid-solid phase transitions below the melting. This was understood as the experimental evidence that alkyl chains are highly disordered in liquid crystalline phases, especially in cubic phases [11]. Although the present specimen of ANBC(22) may be in metastable phase at room temperature as described before, as far as the sample obeys the third law of thermodynamics, entropy is safely compared even in this situation.

Figure 2 suggests that the low-temperature tail of the thermal anomaly below the melting extends down to about 270 K. The normal heat capacity of the solid phase was, therefore, estimated by using the effective frequency distribution method [32] on the basis of the experimental heat capacity data between 70 and 220 K, where no effect of the premelting seems to exist. The resultant normal heat capacity is drawn in Fig. 2 by dotted curve. By integrating the excess heat capacity beyond the normal curve, the enthalpy and enthalpy gains are determined as 37.62 $\mathrm{kJ\,mol^{-1}}$ including the effect of the latent heat (ca. 30 $\mathrm{kJ\,mol^{-1}}$) and 101.89 $\mathrm{J\,K^{-1}\,mol^{-1}}$, respectively. The total excess entropy acquired by the isotropic liquid amounts to 212.2 $\mathrm{J\,K^{-1}\,mol^{-1}}$. The corresponding value is 156.9 $\mathrm{J\,K^{-1}\,mol^{-1}}$ for ANBC(16) [26], 158.2 $\mathrm{J\,K^{-1}\,mol^{-1}}$ for ANBC(18) [12], and 144.2 $\mathrm{J\,K^{-1}\,mol^{-1}}$ for BABH(8) [31]. On the other hand, the excess entropy beyond the contribution from intramolecular vibrations in the isotropic liquid phase is expected to fall within 240–290 $\mathrm{J\,K^{-1}\,mol^{-1}}$ considering the contributions of the core (35–55 $\mathrm{J\,K^{-1}\,mol^{-1}}$) [33] and chain (210–230 $\mathrm{J\,K^{-1}\,mol^{-1}}$) [34]. The experimental value of the excess entropy shows that the alkyl chains are, though not completely, highly disordered in the liquid crystalline phases, in accordance with the fact that the terminal alkyl chain is highly disordered in the cubic phases [28] and behaves similar to a solvent [11].

D. Stiffness of cubic phases

In Fig. 4, a negative jump in heat capacity is recognized at the Sm-$C\rightarrow$cubic (*Im3m*) transition. Indeed, if one smoothly extrapolates heat capacities of both phases, then the cubic phase run below that of the Sm-*C* phase. That is, the heat capacity of the optically isotropic phase is smaller than those of the neighboring liquid crystalline phases. This trend is also found in thermotropics [ANBC(16) [26], ANBC(18) [12], and BABH(8) [31]] and in a lyotropic system ($C_{12}E_6$, water [35]). Since the heat capacity under constant pressure is proportional to the fluctuation of enthalpy, the small heat capacity means that the fluctuation of enthalpy is small in cubic phases.

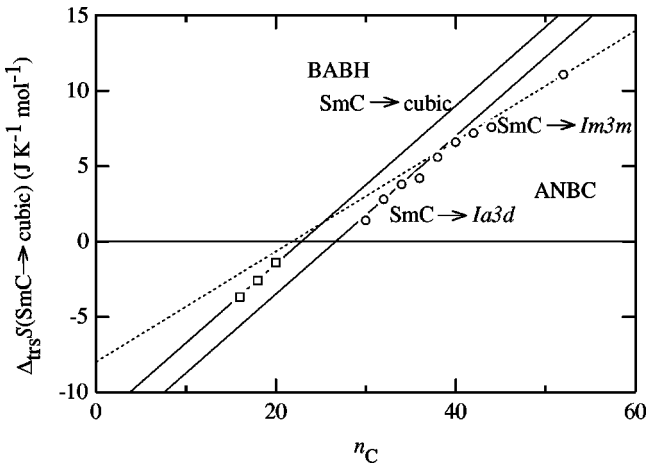

FIG. 6. Entropy of Sm-$C\rightarrow$cubic transition in ANBC(n) and BABH(n). The n_C stands for the number of paraffinic carbon atoms attached to the constituting ''molecule.'' Here the ''molecule'' means a dimer in the case of ANBC and mole is applied to monomer for BABH and dimer for ANBC. The relation $n_C=2n$ holds for both because of its doubled structure of BABH molecule and of dimerization of ANBC molecules.

Lyotropic cubic phases with an interwoven jointed-rod micelle structure, which is nowadays believed to be essentially the same as the structure of the cubic phase of ANBC(16) [10], is often called as viscous liquid because of its viscous property without optical anisotropy. On the other hand, the viscoelastic property of ANBC(n) ($n=15,16,22$) reported previously [37,38] shows that the cubic phases are much stiffer than the neighboring liquid crystalline phases. For both the lyotropic and thermotropic cubic phases, therefore, their smaller heat capacities than those of neighboring liquid crystalline phases are consistent with their bulk stiffness, which suppresses the enthalpy fluctuation.

E. Degree of disorder in Sm-*C*, cubic *Ia3d*, and *Im3m* phases

Figure 6 shows chain-length dependence of entropy of transition from the Sm-*C* phase to the cubic mesophases. For the sake of consistent comparison between more compounds, data obtained using commercial differential scanning calorimeter are selected here [18,24]. The abscissa of the plot (n_C) is the number of paraffinic carbon atoms within a constituent ''molecule.'' Since most ANBC molecules are in a carboxylic acid dimer state [28], the corresponding number is twice of the actual chain length. In Fig. 6, the dependence of BABH(n) (shown in Fig. 1) is also included [30].

Although the discussion on BABH was already given previously [12], we shall briefly repeat here in order to explain our logic. Since the phase sequence in BABH is inverted (cubic $\rightarrow$Sm-*C* on heating), the entropy of transition in Fig. 6 is negative. The entropy of transition is a linear function of n_C with a positive slope and a negative intercept at $n_C=0$. As entropy is an extensive variable having a clear statistical meaning, this positive slope indicates that the chain is more

disordered in the cubic phase than in the Sm-*C* phase. The negative entropy of transition, on the other hand, implies that the core is more ordered in the cubic phase. The intercept provides a measure for the entropy change attributable to the core. It is noted that the partition of entropy made here is on real ''particles'' basis. The contribution of chain, therefore, includes not only that assignable to ''static'' arrangement but also those of vibration, free-volume, and unidentified specific excitation, etc. In the core contribution, beside such contributions, the effect of connectivity between core and chain is included The effective core size may, therefore, be different from the real size of the core part of a molecule.

Next, we shall discuss ANBC. The entropy of transition is an increasing function of n_C. This again indicates that the chain is more disordered in the cubic phase than in the Sm-*C* phase. This is consistent with the reported nuclear magnetic resonance linewidth for ANBC(16) [36]. In a previous paper [12], the presence of two cubic phases in this series, which appear depending on the number of paraffinic carbon atoms, was not known. A straight line was, therefore, drawn by putting more weight on the data with the small carbon number, because a deviation from a linear relation is apparently seen at the longer chain side. We now know that the cubic *Im3m* phase appears for the mesogens with $n_C=38$ [ANBC(19)] and longer, and that the *Ia3d* phase locates at the high-temperature side of the *Im3m* phase [16–18]. A straight line is drawn for the entropy of Sm-$C\rightarrow$*Ia3d* transition for $n_C<40$. This line is essentially the same as the previous line. The slope of this line $[0.54\ \mathrm{J\,K^{-1}}\ (\mathrm{mol\ of\ CH_2})^{-1}]$, therefore, indicates the difference in entropy per paraffinic carbon atom between the Sm-*C* and the *Ia3d* phase. Since it is not likely that long chains such as $C_{14}H_{29}$ do not contribute to the entropy of transition, the presence of some reverse contribution by the core canceling the effect of chains is easily anticipated, as in the case of BABH.

The entropy of the Sm-$C\rightarrow$*Im3m* transition is an increasing function with a smaller slope $[0.36\ \mathrm{J\,K^{-1}}\ (\mathrm{mol\ of\ CH_2})^{-1}]$ than that of the Sm-$C\rightarrow$*Ia3d* transition. This shows that conformation of a chain in the *Im3m* phase is more disordered than in the Sm-*C* phase but less than in the *Ia3d* phase. On the other hand, the relative position of the straight lines of the *Im3m* and *Ia3d* phases implies that the order of the core is higher in the *Ia3d* phase than in the *Im3m* phase. It is not straightforward to determine what extent of the chain from the core is merged in an ''effective core'' responsible for stabilization of the *Im3m* phase. In the case of the *Ia3d* phase [12], its appearance in short-chain ANBCs [11,15] was interpreted on the basis of such estimate, which suggests that $n_C=16$ roughly corresponds to the ''effective core.'' In the case of the *Im3m*, however, such estimate seems to be impossible because we must realize a metastable *Im3m* phase (with respect to the stable *Ia3d* phase). Then, we assume a similar effective core for the *Im3m* phase as in the case of the *Ia3d* phase. The entropy of the Sm-$C\rightarrow$*Im3m* transition assignable to the core is, therefore, estimated as $(-3\pm1)\ \mathrm{J\,K^{-1}}\ (\mathrm{mol\ of\ core})^{-1}$. This is approximately the half of that for the *Ia3d* phase $[(-6\pm2)\ \mathrm{J\,K^{-1}}\ (\mathrm{mol\ of\ core})^{-1}]$. The degree of disorder in the Sm-*C*, cubic *Im3m*, and cubic *Ia3d* phases is schematically shown in Fig. 7. The actual phase sequence in long-chain ANBCs (Sm-$C\rightarrow$*Im3m*$\rightarrow$*Ia3d*) is governed by the chain length.

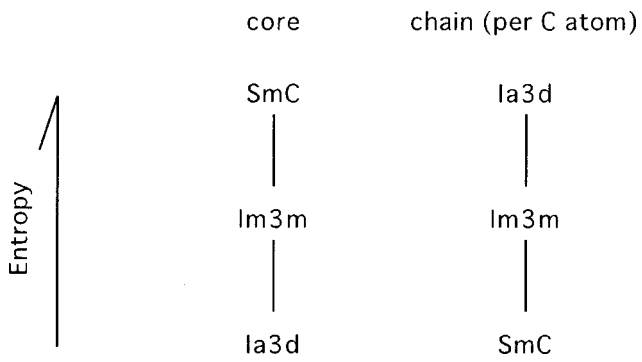

FIG. 7. Entropy relation for core and chain of ANBC among the Sm-*C*, cubic *Im3m*, and *Ia3d* phases.

It is not clear at present whether the slope(s) in Fig. 6 be universal (independent of compounds). As for the cubic phases, the fact that ANBC and BABH give quite similar slopes suggests that the slope be universal for specific phase (not for compound). In this context, researchers having synthetic skills are requested to prepare many compounds with different chain lengths. This enables us, not only for cubic phases but also *for any liquid crystalline phases*, to deduce the intrinsic entropy of transition assignable to molecular shape, which makes it possible to directly compare with many molecular statistical models.

F. Change in phase sequence upon chemical decoration

Since the ''chain'' is common to this type of compounds, only the part we can modify is the core. The origin of the appearance of different cubic phases, at least *Ia3d* and *Im3m* phases, should, therefore, be attributed to difference in core. We now consider a question as to what is the origin of a phase sequence different from compound to compound. We shall suppose that the Sm-*C* phase has the lowest entropy among the three. This assumption seems reasonable because most cubic phases appear at the high-temperature side of the Sm-*C* phase. An exception is BABHs [12,13,29–31]. Depending on chain length and interaction strength in the lateral direction, there are four possibilities for the relationship between Gibbs energy and temperature as shown in Fig. 8. It is likely that stronger stabilization occurs in the more ordered *Ia3d* phase. Enhanced interaction, therefore, changes the phase sequence downward. Namely, the *Ia3d* phase would come first upon heating from the Sm-*C* phase if the lateral interaction is sufficiently strong. Depending on the chain length, on the other hand, the relative magnitude of entropies of the *Ia3d* and *Im3m* phases changes. Elongation of the chain increases the entropy of the *Ia3d* phase. The phase sequence thus changes rightward in Fig. 8. In summary, a compound with weak interaction and short chain shows the phase sequence Sm-$C\rightarrow$*Im3m*, corresponding to the case (a). The *Ia3d* phase is not realized as a stable phase in this case. Contrary to this, a compound with strong interaction

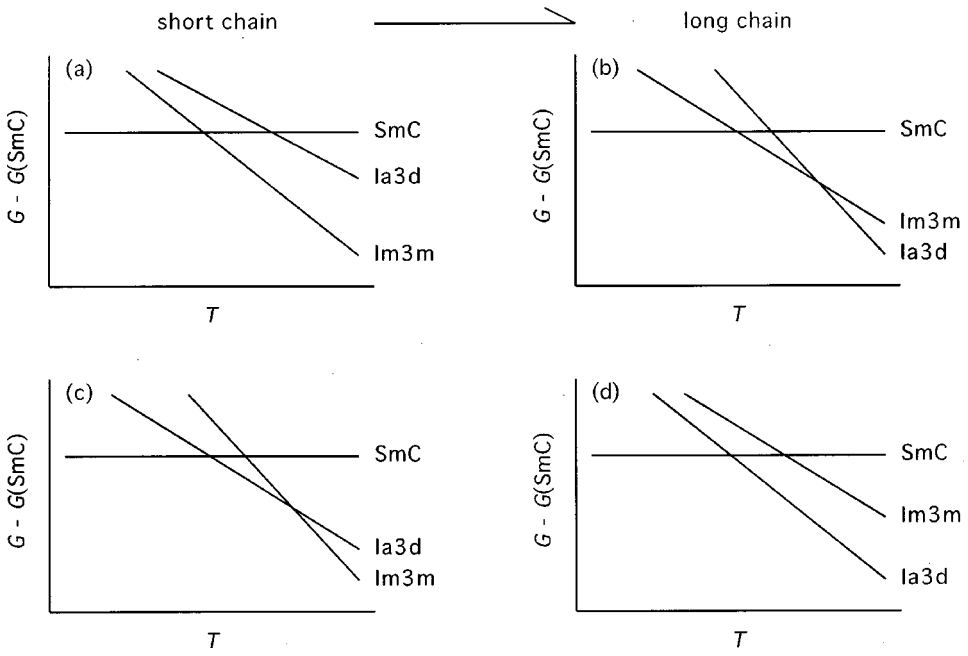

FIG. 8. Gibbs energy (G)-temperature (T) diagrams showing possible phase sequences including two cubic (*Ia3d* and *Im3m*) phases.

and long chain shows the sequence of Sm-$C\rightarrow$*Ia3d*, the case (d). The *Im3m* phase does not appear here.

The long-chain ANBC showing the phase sequence of Sm-$C\rightarrow$*Im3m*$\rightarrow$*Ia3d* corresponds to the case (b) in Fig. 8, while the short-chain ANBC having only the cubic *Ia3d* phase to the case (c) because the entropy of the *Ia3d* phase is smaller than that of the *Im3m* phase as seen from Fig. 6. The shift from (c) to (b) on elongation of the chain is caused by effective weakening of the intermolecular interaction due to the enlargement of the molecule. In reality, the phase sequence changes from the case (c) to (b) through (a) where only the *Im3m* phase appears [17,39].

The cubic phase of ACBC(16) [8] is known to belong to the space group *Im3m* [10]. Namely, ACBC(16) is in the case (a) or (b). On the other hand, the ANBC(16) is of the case (c) and undergoes the Sm-$C\rightarrow$*Ia3d* transition. These two molecules are different only in a substituent group attached to the biphenyl core. This slight change in molecular structure modifies the intermolecular interaction in the lateral direction. Since the molecules have the same alkyl chain, a possible shift is limited to the vertical ones in Fig. 8. Since ANBC(16) is of the case (c), ACBC(16) is naturally assigned to the case (a). This implies that the intermolecular interaction in the lateral direction is stronger in ANBC than in ACBC. This tendency is supported by a larger electric dipole moment produced by the NO_2 group in the ANBC(16) than the CN group in the ACBC(16) molecule.

IV. CONCLUSION

On the basis of ''binary system'' approximation for the cubic mesophases having space group *Ia3d* or *Im3m*, we analyzed the entropy of Sm-$C\rightarrow$cubic phase transition of the homologous series of ANBC, and deduced (semi)quantitatively the degree of disorder among the Sm-C, cubic *Im3m*, and *Ia3d* phases. This method is, in principle, applicable to any liquid crystalline phases of mesogens having a rigid core and long alkyl chain(s), and yields the entropy of transition assignable to the core, which is to be easily compared with molecular-statistical models. By considering possible phases sequences, the change in phase sequence on elongation of the alkyl chain and in the space group on changing the molecule is interpreted. The results derived here serve as a framework for molecular-statistical modeling of these exotic aggregation states of matter.

ACKNOWLEDGMENTS

The authors thank Mr. Tatsuya Ichikawa at Gifu University for his help in preparing the sample. This work was supported in part by a Grant-in-Aid for Scientific Research (A) (11304050) from the Ministry of Education, Culture, Sports, Science, and Technology, Japan.

[1] S. Diele and P. Göring, in *Handbook of Liquid Crystals*, edited by D. Demus, J. Goodby, G. W. Gray, H.-W. Spiess, and V. Vill, Low Molecular Weight Liquid Crystals II (Wiley-VCH, Weinheim, 1998), Chap. XIII.
[2] U. S. Schwarz and G. Gompper, Phys. Rev. E **59**, 5528 (1999).
[3] A. D. Benedicto and D. F. O'Brien, Macromolecules **30**, 3395 (1997).
[4] L. Onsager, Ann. N.Y. Acad. Sci. **51**, 627 (1949).
[5] S. Chandrasekhar, *Liquid Crystals*, 2nd ed. (Cambridge University Press, Cambridge, 1992).
[6] P. G. de Gennes and J. Prost, *The Physics of Liquid Crystals*, 2nd ed. (Clarendon Press, Oxford, 1993).
[7] G. W. Gray, B. Jones, and F. Marsond, J. Chem. Soc. 393 (1957).

[8] D. Demus, G. Kunicke, J. Neelsen, and H. Sackmann, Z. Naturforsch. A **23**, 84 (1968).
[9] G. W. Gray and J. W. Goodby, *Smectic Liquid Crystals – Textures and Structures* (Leonard Hill, Glasgow, 1984), Chap. 4, and references therein.
[10] A.-M. Levelut and M. Clearc, Liq. Cryst. **24**, 105 (1998).
[11] K. Saito, A. Sato, and M. Sorai, Liq. Cryst. **25**, 525 (1998).
[12] A. Sato, Y. Yamamura, K. Saito, and M. Sorai, Liq. Cryst. **26**, 1185 (1999).
[13] K. Saito, A. Sato, N. Morimoto, Y. Yamamura, and M. Sorai, Mol. Cryst. Liq. Cryst. Sect. A. **347**, 249 (2000).
[14] K. Saito, T. Shinhara, and M. Sorai, Liq. Cryst. **27**, 1555 (2000).
[15] K. Morita, S. Yano, S. Kutsumizu, and S. Nojima, in *Japan Liquid Crystal Conference, 2000 Matsue, Japan, 2000* (Japanese Liquid Crystal Society, Tokyo, 2000), Abstract Pab04.
[16] S. Kutsumizu, T. Ichikawa, S. Nojima, and S. Yano, Chem. Commun. (Cambridge) 1181 (1999).
[17] S. Kutsumizu, T. Ichikawa, S. Nojima, and S. Yano, in *18th International Liquid Crystalline Conference, Sendai,Japan, 2000* (Japanese Liquid Crystal Society, Tokyo, 2000), Abstract 27c-7-0
[18] S. Kutsumizu, T. Ichikawa, M. Yamada, S. Nojima, and S. Yano, J. Phys. Chem. B **104**, 10196 (2000).
[19] M. Sorai, K. Kaji, and Y. Kaneko, J. Chem. Thermodyn. **24**, 167 (1992).
[20] T. Preston-Thomas, Metrologia **27**, 107 (1990).
[21] See EPAPS document No. E-PLEEE8-65-124203 for numerical tables of heat capacity data and standard thermodynamic quantities (heat capacity, enthalpy, entropy, and Gibbs energy) at round temperatures of ANBC(22). This document may be retrieved via the EPAPS homepage (http://www.aip.org/pubserves/epaps.html) or from ftp.aip.org in the directory /epaps/; see the EPAPS homepage for more information.
[22] L. D. Landau and E. M. Lifshitz, *Statistical Physics*, 3rd ed. Part 1 (Pergamon Press, New York, 1980), Chap. XIV.
[23] H. T. Stokes and D. M. Hatch, *Isotropy Subgroups of the 230 Crystallographic Space Groups* (World Scientific, Singapore, 1988).
[24] S. Kutsumizu, M. Yamada, and S. Yano, Liq. Cryst. **16**, 1109 (1994).
[25] J. W. Goodby, D. A. Dunmur, and P. J. Collings, Liq. Cryst. **19**, 703 (1995).
[26] A. Sato, K. Saito, and M. Sorai, Liq. Cryst. **26**, 341 (1999).
[27] A. S. Coolidge, J. Am. Chem. Soc. **50**, 2166 (1928).
[28] S. Kutsumizu, R. Kato, M. Yamada, and S. Yano, J. Phys. Chem. B **101**, 10 666 (1997).
[29] H. Schubert, J. Hauschild, D. Demus, and S. Hoffmann, Z. Chem. **18**, 256 (1978).
[30] D. Demus, A. Gloza, H. Hartung, A. Hauser, I. Rapthel, and A. Wiegeleben, Cryst. Res. Technol. **16**, 1445 (1981).
[31] N. Morimoto, K. Saito, Y. Morita, K. Nakasuji, and M. Sorai, Liq. Cryst. **26**, 219 (1999).
[32] M. Sorai and S. Seki, J. Phys. Soc. Jpn. **32**, 382 (1972).
[33] G. W. Smith, Mol. Cryst. Liq. Cryst. **49**, 207 (1979).
[34] M. Sorai, K. Tsuji, H. Suga, and S. Seki, Mol. Cryst. Liq. Cryst. **80**, 33 (1980).
[35] M. Nishizawa, K. Saito, and M. Sorai, J. Phys. Chem. B **105**, 2987 (2001).
[36] P. Ukleja, R. E. Siatkowski, and M. E. Neubert, Phys. Rev. A **38**, 4815 (1988).
[37] T. Yamaguchi, M. Yamada, S. Kutsumizu, and S. Yano, Chem. Phys. Lett. **240**, 105 (1995).
[38] S. Kutsumizu, T. Yamaguchi, R. Kato, and S. Yano, Liq. Cryst. **26**, 567 (1999).
[39] S. Kutsumizu *et al.* (unpublished).